

Numerical modelling assessment of climate-change impacts and mitigation measures on the Querença-Silves coastal aquifer (Algarve, Portugal)

Rui Hugman¹ · Tibor Stigter² · Luis Costa¹ · José Paulo Monteiro¹

Received: 17 August 2016 / Accepted: 3 April 2017 / Published online: 6 May 2017
© Springer-Verlag Berlin Heidelberg 2017

Abstract Predicted changes in climate will lead to seawater intrusion in the Querença-Silves (QS) coastal aquifer (south Portugal) during the coming century if the current water-resource-management strategy is maintained. As for much of the Mediterranean, average rainfall is predicted to decrease along with increasing seasonal and inter-annual variability and there is a need to understand how these changes will affect the sustainable use of groundwater resources. A density-coupled flow and transport model of the QS was used to simulate an ensemble of climate, water-use and adaptation scenarios from 2010 to 2099 taking into account intra- and inter-annual variability in recharge and groundwater use. By considering several climate models, bias correction and recharge calculation methods, a degree of uncertainty was included. Changes in rainfall regimes will have an immediate effect on groundwater discharge; however, the effect on saltwater intrusion is attenuated by the freshwater–saltwater interfaces’ comparatively slow rate of movement. Comparing the effects of adaptation measures demonstrates that the extent of intrusion in the QS is controlled by the long-term water budget, as the effectiveness of both demand and supply oriented measures is proportional to the change in water budget, and that to maintain the current position, average groundwater discharge should be in the order of $50 \times 10^6 \text{ m}^3 \text{ yr}^{-1}$.

Keywords Numerical modelling · Salt-water/freshwater relations · Resource management · Coastal aquifers · Portugal

✉ Rui Hugman
rthugman@gmail.com

¹ Universidade do Algarve, Faro, Portugal

² UNESCO-IHE, Delft, The Netherlands

Introduction

The Mediterranean countries have an area around 8.82 million km² and a population of about 420 million. Of these, about 37% live in the coastal strip, and the situation is reinforced by a seasonal, tourist and migratory flow of more than 100 million people (MED-EUWI 2007). Freshwater availability in the Mediterranean region is under increasing pressures from water-consuming and contaminating activities which threaten drinking water and irrigation supplies (Stigter et al. 2013). Current predictions indicate that climate change will contribute to aggravate these pressures, with decreasing rainfall and longer and more frequent drought periods (Giorgi 2006; IPCC 2014). Managing these freshwater reserves is an increasingly important issue, in particular for coastal areas due to the added threat of contamination from saline waters (Custodio 2002). Coastal aquifers can also represent a significant portion of the freshwater discharge to the sea, as well as being an important pathway for nutrient and contaminant transport to coastal marine areas (Burnett and Aggarwal 2006). Understanding coastal discharge is also important from a water-resource-management perspective. The extent of seawater intrusion (SWI) or submarine groundwater discharge (SGD) at a given location is essentially an issue of balance between fresh and seawater pressures (Taniguchi et al. 2002). As such, managers require knowledge of coastal discharge to assess the volume of fresh water lost to the sea, and therefore unavailable for pumping, and it makes sense to consider and quantify SGD and SWI when discussing the management of coastal groundwater reserves (note: abbreviations are given in the Appendix).

SWI in coastal aquifers is a common problem in areas where water supply is dependent on groundwater (Custodio 2002) and is often particularly severe in semi-arid and arid areas where recharge is low (Abarca et al. 2007). The balance

between freshwater and saltwater can be disrupted by natural (e.g. droughts/floods) or anthropogenic causes (e.g. abstraction, soil impermeabilization), which can cause seawater to move towards or away from land. Concern over climate change has stimulated research on the expected impacts on groundwater systems during the last few years, reviews of which can be found in Green et al. (2011) and Taylor et al. (2012). The impact of climate change on seawater intrusion has mostly been focused on theoretical studies of boundary condition (BC) controls on SWI processes using simplified numerical and analytical models (e.g. Werner and Simmons 2009; Watson et al. 2010; Chang et al. 2011; Ferguson and Gleeson 2012; Chang and Clement 2012) and site specific assessments (e.g. Carneiro et al. 2010; Payne 2010; Oude Essink et al. 2010; Rozell and Wong 2010; Loáiciga et al. 2012; Sulzbacher et al. 2012; Rasmussen et al. 2012; Green and MacQuarrie 2014). These studies mostly carry out simulations for a range of combinations of predicted sea-level rise (Loáiciga et al. 2012), change in recharge (Carneiro et al. 2010; Payne 2010; Rozell and Wong 2010; Green and MacQuarrie 2014) and surface-water elevation (Oude Essink et al. 2010; Rasmussen et al. 2012), applying average long-term values without considering inter-annual or seasonal variability. However, Michael et al. (2005) have shown that seasonal recharge causes the freshwater–saltwater interface to oscillate seasonally. Yet, few or no studies have taken into account the impact of expected changes in recharge regimes on SWI and SGD.

Studies of the impact of climate change incorporate several sources of uncertainty: carbon dioxide emission and socioeconomic scenarios (IPCC 2014), selected circulation models and applied downscaling methods (Holman 2006; Jackson et al. 2011). Error inherent to methods used to translate climate data into runoff or recharge (e.g. soil-water balance models, 1-D variably saturated flow models and empirical relationships) can introduce further uncertainty, as they can respond differently to temporal variations in rainfall, whilst providing similar long-term averages (Holman et al. 2012). In their guide to best practises for groundwater climate change studies, Holman et al. (2012) suggest that analyses should include a range of scenarios that take all these sources of uncertainty into account. This of course requires a large number of model runs, which can be problematic when dealing with computationally expensive models required to simulate coastal aquifer dynamics.

Groundwater in the Algarve region (south of Portugal), as in most of the Mediterranean basin, is under growing pressure from the combined effect of rising sea level, reduced rainfall and increasing crop water demand caused by global warming (Giorgi 2006; Santos and Miranda 2006). Water management policy needs to adapt to this changing environment in order to guarantee water supply as well as maintain the sustainability of the resource and other dependent systems. The Querença-

Silves (QS) is a coastal aquifer and one of the main sources of freshwater supply for irrigation in the region, as well as serving as a backup to the public water supply system during prolonged droughts (Stigter et al. 2009). Stigter et al. (2013, 2014) have shown that climate change will have significant impacts on groundwater levels and spring discharge rates of this aquifer. Apart from the reduced availability of groundwater for anthropogenic use, changes in discharge to springs and streams will have impacts on sensitive groundwater dependent ecosystems (Silva et al. 2012). Previous studies have shown that the intensification of seasonality has a significant effect on the sustainable level of exploitation when considering freshwater discharge to the coast (Hugman et al. 2012, 2013); however, so far the impact on SWI has not been extensively explored.

The aim of this study is to determine the potential for SWI in the QS aquifer system for a range of climate change and groundwater use and adaptation scenarios, as well as to assess the impact of seasonal variability on the extent of SWI. An ensemble of climate scenarios previously developed by Stigter et al. (2014) are applied to a local-scale cross-sectional coupled-density flow and transport model. Results incorporate uncertainty from climate modelling by including input from three climate models, two downscaling methods and two soil-water budget methods to determine monthly recharge rates and crop water demand. Innovative aspects include the simulation of seasonal and inter-annual variation and assessment of the impact of changes in recharge regimes on SWI. Identified adaptation measures are subsequently simulated for the worst-case climate scenario to determine their relative effectiveness in reducing SWI.

Study area: Querença-Silves (M5) aquifer system

The QS aquifer system (Figs. 1 and 2) is a karstified carbonate rock aquifer formed by Jurassic (Lias-Dogger) carbonate sedimentary rocks, that extends over an irregular area of 324 km² from the Arade River (in the west) to the village of Querença (in the east; Almeida et al. 2000; Monteiro et al. 2006, 2007a). As the largest aquifer in the Algarve (south Portugal) and the amount of recharge it is the most significant groundwater reservoir in the region.

The system is limited to the south by the Algibre thrust, the main onshore thrust in the Algarve Basin, separating the Lower/Early and the Upper/Late Jurassic, and to the north by Carboniferous shale and greywacke. Flow is mainly from east to west, with the main natural discharge area at the Estombar springs along the estuary of the Arade River. These springs support important and sensitive surface/groundwater ecotones, many of which are classified as protected areas (Silva et al. 2012). Several streams cross the system from north to south and switch between being gaining

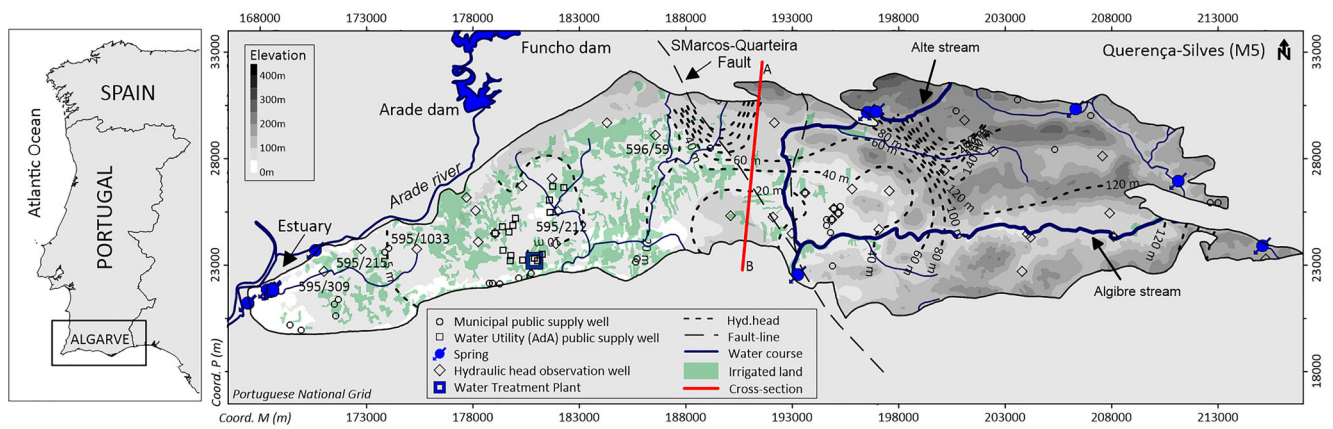


Fig. 1 Location and main features of the Querença-Silves aquifer system

and loosing along their path. Salvador et al. (2012) provided an initial attempt to quantify and simulate these exchanges; however, further work is necessary to comprehend the complex nature of these surface/groundwater interactions.

The aquifer is divided into two compartments, evidenced by both the distinct change in topography (Fig. 1) and temporal variation of hydraulic head measured in piezometers (Fig. 3). Flow patterns in the east are complex, whilst in the west they indicate a well-connected karst with a clear east to west flow path. Recently Neves et al. (2016) explored the temporal structure of a groundwater-level time series in the QS, confirming the distinct nature of the two sectors. They found that the western sector displays characteristics consistent with relatively large and uniform values of water storage capacity and transmissivity properties, while the eastern sector shows larger spatial and temporal heterogeneity. Despite being a karst system, the regional piezometry of the QS, characterized by low gradients in the western sector, and the hydraulic head fluctuations denote the existence of a well-developed conduit network controlling flow at a regional level. Thus,

conduit flow may have local-scale effects, but the regional flow patterns are relatively homogeneous.

Groundwater quality in the region is monitored by the Portuguese Environmental Agency with an extensive network of wells, boreholes and springs. Average chloride concentrations observed near the discharge area of the QS are presented in Fig. 4a. Chloride concentrations are low for most of the system, increasing in the proximity of the Arade estuary. Highest values are measured at the Estombar springs and well 595/262, which is in the vicinity of the springs. Figure 4b presents time series of chloride measurements for selected wells. Unfortunately, observations are sparse; however, they do suggest that chloride concentrations in spring discharge increased during the 2004/2005 drought and continued high during the subsequent years. Of note is the spike in concentration associated to the large increase in groundwater levels in the winter of 2009, and subsequent improvement in water quality. In fact this occurs in every annual cycle, with chloride concentrations increasing with the rise in water levels at the beginning of the wet season. It is likely that the increase in

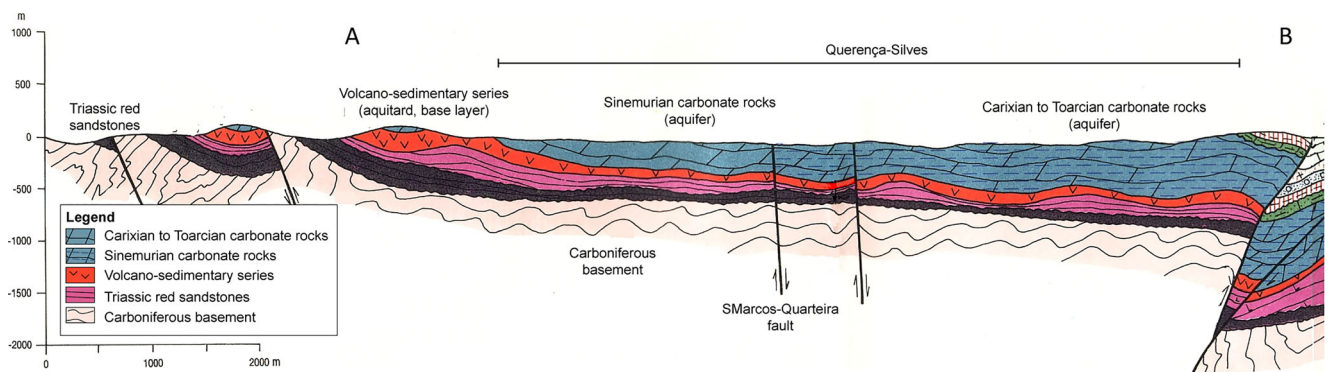


Fig. 2 Geological cross section of the QS aquifer. Aquifer series: Sinemurian and Carixian to Toarcian carbonate rocks; Aquitard and basement formations: Volcano-sedimentary series and Carboniferous basement. Location of cross-section is shown in Fig. 1. (Adapted from Manuppella (1992))

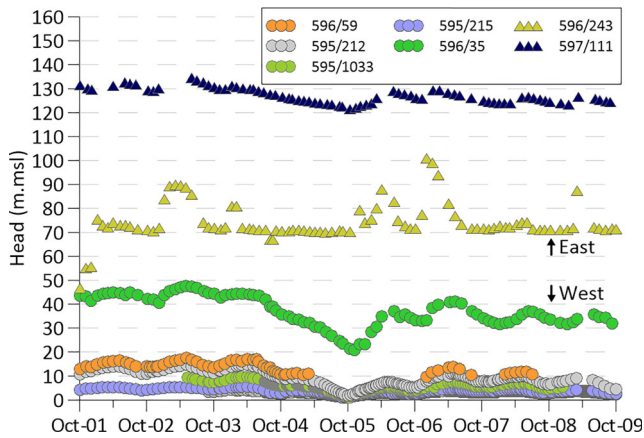


Fig. 3 Selected groundwater level time series registered by the regional water management monitoring network from 2001 to 2009

freshwater flow serves to flush saltwater that intruded during the prior dry period, lagging behind the recharge event.

Climate

The region has a warm Mediterranean climate, and the coastal zone is considered semi-arid due to the precipitation to potential evapotranspiration ratio (Estrela et al. 1996). Rainfall is irregular, characterized by long dry summer seasons and heavy rainfall periods during the winter months, as well as large seasonal and annual variability (Stigter et al. 2009). Average annual rainfall and temperature are 650 mm and 17 °C respectively.

Current predictions are for an increase in frequency and intensity of droughts in the future (Giorgi 2006; Santos and Miranda 2006). Mean annual rainfall in the Algarve is expected to decrease slightly up to 2050; however, significant reductions in rainfall are expected towards the end of the century (Stigter et al. 2014). The most significant expected change in the short-term are shifts in seasonal distribution and inter-annual variability, with a greater concentration of rainfall in the winter season and large reductions in spring and autumn (Stigter et al. 2014).

Recharge

Monteiro et al. (2006) originally estimated mean annual recharge for the QS at $93 \times 10^6 \text{ m}^3 \text{ yr}^{-1}$ (287 mm yr⁻¹). Oliveira et al. (2008) applied the Food and Agriculture Organization (FAO) dual crop coefficient method using a sequential daily water balance model (BALSEQ_MOD), and obtained average annual recharge rates of $104 \times 10^6 \text{ m}^3 \text{ yr}^{-1}$ (321 mm yr⁻¹) along with a detailed spatial distribution of recharge.

Recent research by Stigter et al. (2009, 2014) on climate scenarios and their impacts on groundwater resources and dependent ecosystems in the Central Algarve, show that mean annual rainfall is expected to decrease slightly within the next 50 years (Tables 1). The most significant change will be an increase in seasonal and inter-annual variability, with rainfall concentrated in the winter season, and large reductions in spring and autumn. Hugman et al. (2012, 2013) have shown that this increased seasonality will contribute to reducing the systems resilience to droughts and other extreme events. Within the next 100 years, a significant decrease in both rainfall and recharge is predicted.

Groundwater use

Up to the end of the twentieth century, public water supply in the Algarve was managed at a municipal scale and was almost entirely dependent on groundwater. Lack of regional planning and unregulated groundwater use gave origin to a range of quantitative and qualitative problems (Monteiro and Costa 2004). Along with increasing water demand, these problems lead to the implementation of a water policy based on developing large surface water reservoirs, which now supply most public water demand in the Algarve. However, the severe drought of 2004/2005 highlighted the fragility of this single source supply scheme and has been caused a push towards an integrated water-resource management (Stigter et al. 2009).

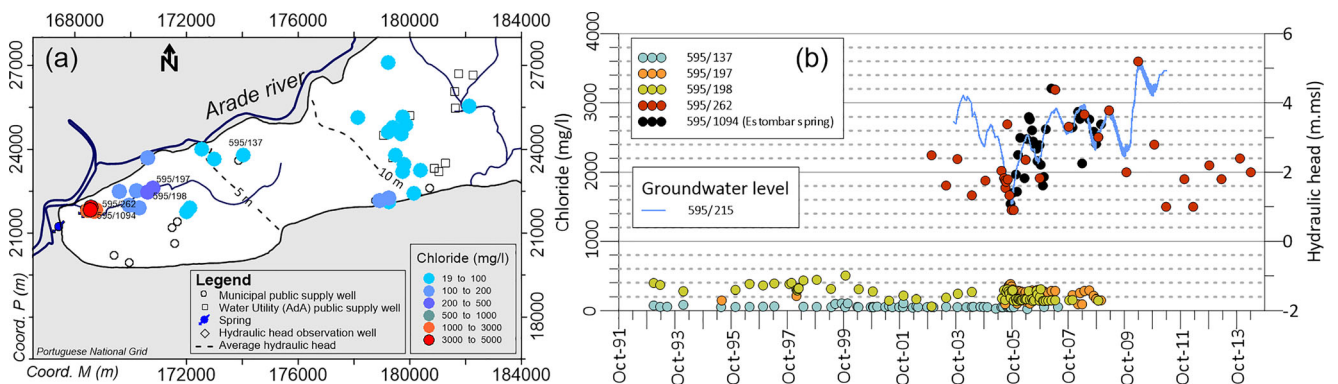


Fig. 4 a Groundwater quality monitoring network and average observed chloride concentration; b time series of chloride concentration measured at selected stations

Table 1 Estimated mean annual values for rainfall, recharge and crop water demand; average results for an ensemble of climate scenarios (adapted from Stigter et al. 2014)

Parameter	Current		2020–2050			2069–2099		
			Absolute value		Change	Absolute value		Change
	mm yr ⁻¹	×10 ⁶ m ³ yr ⁻¹	mm yr ⁻¹	×10 ⁶ m ³ yr ⁻¹		mm yr ⁻¹	×10 ⁶ m ³ yr ⁻¹	
Rainfall	739	239	685	222	-7%	526	170	-29%
Total recharge	340	110	323	105	-5%	206	67	-39%
Net recharge	246	80	216	70	-12%	82	27	-67%
Crop groundwater demand	94	30	107	35	14%	124	40	32%

The main pressure on groundwater resources in the QS comes from agriculture. Nunes et al. (2006) estimated an annual withdrawal of $31 \times 10^6 \text{ m}^3 \text{ yr}^{-1}$ for irrigation, mostly located in the western part of the aquifer system (see Fig. 1). Current groundwater abstraction for public supply is managed entirely by the regional water utility and is in the order of 4 to $10 \times 10^6 \text{ m}^3 \text{ yr}^{-1}$. Prior to 1999, well fields operated by municipal councils withdrew around $12 \times 10^6 \text{ m}^3 \text{ yr}^{-1}$ (Monteiro et al. 2006). The period with highest abstraction occurred during the 2004/2005 drought, when municipal councils were forced to re-activate their wells. An estimated $26.5 \times 10^6 \text{ m}^3 \text{ yr}^{-1}$ of groundwater was used for public supply during this period (Monteiro et al. 2006).

Materials and methods

Numerical method

Solving density-coupled flow and transport problems requires the solution of a complex system of coupled non-linear partial differential equations (Smith and Turner 2001). This system is solved here using the finite element method, as applied within the commercial modelling software FEFLOW (Diersch 2014). Detailed descriptions of the governing equations and theoretical development and benchmarking of the FEFLOW code can be found in Kolditz et al. (1998), Diersch and Kolditz (1998) and Diersch (2014).

The general form of the partial differential equation for variable-density groundwater flow in saturated porous media (Eq. 1) can be expressed as:

$$\rho S_p \frac{\partial p}{\partial t} + \theta \frac{\partial \rho}{\partial c} \frac{\partial c}{\partial t} = -\nabla \cdot \left[\rho \frac{\mathbf{k}}{\mu} (\nabla p - \rho \mathbf{g}) \right] + \bar{\rho} q_s \quad (1)$$

where ρ is the density of the fluid [ML^{-3}], S_p is the specific storage in terms of pressure [$\text{LT}^{-2} \text{M}^{-1}$], t is time [T], p is pore pressure [$\text{ML}^{-1} \text{T}^{-2}$], θ is porosity [-], c is solute concentration [ML^{-3}], \mathbf{k} is the permeability tensor [L^2], $\bar{\rho}$ is the density of water entering/leaving from a sink/source [ML^{-3}], and q_s is

the volumetric flow rate per unit volume of aquifer representing sources and sinks [T^{-1}]. On the left, the first term is rate of fluid mass accumulation due to pore pressure change and the second term is rate of fluid mass accumulation due to the change in solute concentration. If density is constant, this last term cancels. The representation of the flow domain of karst systems as a single continuum equivalent porous media (EPM) is valid when modelling processes at a regional scale (Scanlon et al. 2003). At a local scale, the presence of fractures and karstic features can have a significant effect on the distribution of flow and transport and require fracture network or dual porosity modelling approaches to be adequately simulated. However, these approaches require a large amount of information on the geometry and hydraulic parameters that can only be obtained in certain cases and is subject to a large amount of uncertainty (Papadopoulou et al. 2010). The lack of detailed data, scale of the system and focus on overall assessment of groundwater resources (as opposed to a need for detailed assessment of localized effects of SWI) makes the EPM approach particularly applicable to the current study.

Groundwater flow is often simulated using Eq. (1) and assuming that density, viscosity, porosity and permeability are constant, in which case it is a differential equation for p and can be solved numerically if certain boundary and initial conditions are specified (Diersch and Kolditz 1998).

Excluding exceptional cases, characteristics of the porous medium are usually not influenced by the flow (e.g. porosity may change under higher pressure or dissolution processes), making the preceding assumption valid; however, viscosity and density are affected by changes salinity or temperature gradients. Thus, for cases in which these are variable, the solution of Eq. (1) requires equations of state linking density and viscosity to solute concentration, whereas for seawater, the relationship between concentration and density can be expressed by a linear empirical relationship, such as:

$$\rho = \rho_s \left[1 + \left(\frac{\rho_s - \rho_f}{\rho_f} \right) \frac{c}{c_s} \right] \quad (2)$$

where ρ_s and ρ_f are saltwater and freshwater density [ML^{-3}] respectively and c_s is the reference concentration of seawater. The change in solute concentration between freshwater and seawater is insufficient to cause significant effects on viscosity, which is therefore usually ignored for such problems.

Solute mass is transported in porous media by groundwater flow (advection), molecular diffusion and mechanical dispersion and is described by the following partial differential equation (Zheng and Bennett 1995):

$$\frac{\partial}{\partial t}(\theta R \rho c) = \nabla \cdot [\rho(-\mathbf{q}c + \theta \mathbf{D} \nabla c)] + q_c \quad (3)$$

where R is the retardation factor [–] and \mathbf{D} is the general dispersion tensor [L^2T^{-1}]. The left side describes temporal change of mass, in which the retardation factor, R , can usually be omitted in salt transport problems as the main components interact only slightly with the solid matrix (thus $R \approx 1$). On the right side, the first term describes advection, the second stands for diffusion and dispersion and the final term accounts for sources and sinks.

The hydrodynamic dispersion coefficient tensor includes the processes of molecular diffusion, longitudinal and transverse dispersion and is defined by (Bear 1972):

$$\mathbf{D} = (D_{ij}) = \left[(D + \alpha_T u) \delta_{ij} + (\alpha_L - \alpha_T) \frac{u_i u_j}{u} \right] \quad (4)$$

D is diffusivity [L^2T^{-1}], α_L and α_T longitudinal and transverse dispersivity [L], u_i and u_j are velocity in i and j direction [L^2T^{-1}], u is the flow velocity [L^2T^{-1}].

The coupled solution of Eqs. (1) and (2) describes variable density fluid flow and solute transport. The entire set is difficult to solve and most modellers use simplifications suitable for their specific problems (Diersch and Kolditz 1998). Here the Oberbeck-Boussinesq assumption is applied, which states that changes in density can be neglected except for the buoyancy term in Darcy's Law. This is only valid for cases in which the density variations throughout the system remain relatively small in comparison to the reference density, and as such is not valid for high concentration brines but is applicable to modelling interactions between fresh and seawater in coastal aquifers.

Horizontal plane model: regional scale flow

Prior research at the University of the Algarve has led to the development of a large-scale two-dimensional (2D) horizontal plane model of the QS aquifer system. An in-depth review of the calibration, validation and previous applications can be found in Hugman et al. (2012, 2013), Salvador et al. (2012). This model has previously been applied by Stigter et al. (2014) to run an ensemble of climate change scenarios to assess the impact of anthropogenic use on resource availability and groundwater dependent ecosystems.

The defined conceptual flow model was translated to a finite element mesh with 11,663 nodes and 22,409 triangular finite elements taking into account the geometry of the system and main hydrogeological features. Recharge is spatially distributed according to recharge rates calculated by Oliveira et al. (2008), using the sequential daily water balance model BALSEQ_MOD. An estimated annual abstraction for irrigation of $31 \times 10^6 \text{ m}^3$ (Nunes et al. 2006) is distributed uniformly over 150 nodes, corresponding to wells within agricultural areas. Transient simulations consider abstraction for irrigation only between the last week of May and the end of September. Withdrawals for public supply are applied to nodes corresponding to wells belonging to the regional water utility—Águas do Algarve (AdA)—and municipal councils, who provide monthly abstraction rates. Constant head boundary conditions, equal to mean sea level, were assigned to nodes along the Arade estuary to represent the system's main discharge area. Discharge also occurs from several springs in the central and eastern sections of the system; however, model variants based on these conditions revealed a minor impact on the regional flow pattern and water balance.

Cross-section model: density-coupled flow and mass transport

The computational burden of solving this system, and the need for high spatial and temporal resolutions of the finite element mesh and time-stepping schemes to guarantee numerical stability, often makes the development of large-scale three-dimensional (3D) models impractical (Oude Essink 2001). As the western section of the QS is relatively uniform, with little lateral variation, a simplified 2D cross-section representation was considered sufficient to provide a representation of the interaction between fresh and saltwater within the aquifer. Due to local-scale heterogeneity, the QS behaves as both a confined and unconfined aquifer system in different areas; furthermore, in fractured (or karst) aquifers, the concept of phreatic or confined is not applicable in the usual sense. Even if there is a regional phreatic level in equilibrium with the atmosphere, fractures at depth can be under pressure. This can be visualized considering an inclined fracture that passes through the contact between the saturated and unsaturated zones. At all elevations below this contact, the fracture is under pressure, and if intercepted by a well, it is elasticity that causes water level in the well to rise (as occurs in a confined aquifer).

However, FEFLOW requires a full unsaturated-flow model in order to take into account variably saturated conditions in a 2D cross section model, which would require further parameters to be assigned and significantly increase model run-times. Thus, the model was treated as a fully confined system in order to simplify development and reduce computation time. The previously developed horizontal plane model also

assumed this simplification, applying calibrated storage coefficient values for unconfined conditions (i.e. Hugman et al. 2012; Stigter et al. 2009), which was considered acceptable as model results match observed data reasonably well. Model results may be less accurate when simulating local-scale effects near wells; however, the regional-scale flow patterns are not likely to be unaffected. Notwithstanding, it would be interesting for future work to assess the impact of these simplifications on simulated results.

The representative cross-section model extends 23.5 km from the Arade estuary to the S. Marcos-Quarteira fault line, and a further 500 m into the estuary. To simplify construction, the modelled domain was considered to have an average width of 5 km. A 3D geological model of the system, developed by Monteiro et al. (2007b), was used to define the lower boundary of the model. The upper boundary was determined from maximum observed head values. A finite-element mesh was generated with 37,412 triangular finite elements and 19,888 nodes. The characteristic length of elements is equal to or less than 20 m to guarantee numerical stability. All simulations were run using a forward Euler/backward Euler (FE/BE) time integration scheme for automatic time-step control, as recommended for variable density problems by Diersch (2014), with a maximum time-step of 1 day.

Imposed flow BC (2nd type, Neuman) are used to represent direct recharge from rainfall within the modelled domain and lateral flow from the north-eastern section of the QS system (along the eastern vertical border). Imposed flow rates are obtained from the plane model for both steady-state and transient model runs. Abstraction for irrigation within the modelled domain is distributed across 12 well BCs, roughly scattered according to the spatial distribution of irrigated land; withdrawals for public water supply are grouped into five representative well fields and imposed on well BCs at the approximate distance of these fields from the estuary.

The estuary is represented with constant freshwater head conditions along the top and lateral limit of the model in the west. Equivalent freshwater head values are determined according to Eq. (5):

$$h_f = h_s + \frac{(\rho_s - \rho_f)}{\rho_f} \cdot (h_s - z) \quad (5)$$

in which, h_f is equivalent freshwater head [L], h_s is saltwater head [L], ρ_s [ML⁻³] and ρ_f [ML⁻³] are salt-water density (1,025 kg m⁻³) and freshwater density (1,000 kg m⁻³) respectively and z is elevation of the node [L] (Diersch 2014).

For mass transport, boundary nodes corresponding to the estuary were assigned a relative chloride concentration value ($C_{\max} = 1$), representing 100% fraction of seawater. A boundary constraint condition, in which the presence of a constant chloride concentration is defined according to the flux direction, was included to allow for the formation of an outflow

face. Thus, when mass-flux is positive (entering the system) the constant mass BC is maintained, whilst when it is negative (leaving the system) the chloride concentration is computed and automatically assigned as a flux-BC (Diersch and Kolditz 1998; Diersch 2014). This technique has previously been applied for use in large-scale models (i.e. Kopsiaftis et al. 2009; Nocchi and Salleolini 2013).

Several zones of uniform hydraulic conductivity (K) were defined and the ratio between vertical (K_v) and horizontal (K_h) conductivity assumed to be 0.1. An initial approximation of K was obtained using a flow model under steady-state conditions and PEST (Doherty 2002) to adequately represent values of average hydraulic head at selected monitoring wells. Subsequently, transport and density effects were included and K was refined through trial-and-error. Values of K for the various zones are relatively uniform (± 100 m d⁻¹), except for at the discharge area where it was consistently higher (259 m d⁻¹). Higher conductivity at the discharge area is reasonable in carbonate rocks, which are soluble in water. Groundwater flow may dissolve the limestone, thus increasing the hydraulic conductivity of the aquifer. The amount of dissolution depends mainly on the magnitude of the groundwater flow (Kiraly 1975). As all flow within the QS is channelled through the discharge zone, it is reasonable to assume that this area is subject to the most karstification.

A uniform value (0.00025) for specific storage (S_s) was calibrated by trial-and-error for the period from October 2001 to October 2009. Initial conditions for head and mass were obtained by allowing the model at equilibrium to drain (by deactivating the recharge BC), until it reached groundwater levels representative of the end of summer in 2001.

There is a lack of data on dispersion parameters for the QS. Values for molecular diffusion (10^{-9} m² s⁻¹) and longitudinal and transverse dispersivity (20 and 2 m, respectively) were selected as a compromise between values suggested in the literature for aquifer type and scale (Gelhar et al. 1992; Neuman 2005) and finite-element size. Lower dispersivity values lead to increased numerical instability and oscillations in the results, whilst refining the mesh further would lead to a significant increase in computation time. A uniform value of 0.3 was assumed for porosity. The impact of porosity on the results was assessed by running simulations at the extreme range of physically acceptable values (0.05 and 0.6).

Climate change scenarios

Climate scenarios have previously been developed for the study area by Stigter et al. (2014) as part of larger analysis of the effect of climate change on coastal aquifers in the Mediterranean. These authors obtained temperature and rainfall data from scenarios from the ENSEMBLES project (van der Linden and Mitchell 2009), that result from the combination of a regional climate model (RCM) and a global

circulation model (GCM), with a 25×25 km resolution and a balanced CO₂ emission scenario A1b. Three climate models cover the study area and period up to 2100: CNRM-RM5, C4IRCA3 and ICTP-REGCM3. Obtained data were bias corrected using a control period from 1980 to 2010. Two approaches were applied, in order to compare their applicability and include method uncertainty in the results: (1) calculation of anomalies and (2) monthly linear regression between observed and simulated values. Bias-corrected values were then applied to develop total and net (taking into account crop water demand) groundwater recharge scenarios, using the soil-water budget. The sensitivity of the results to the choice of soil-water budget method was assessed by comparing the results using the Thornthwaite-Mather (TM) and Penman-Grindley (PG) methods. The differences between the two methods were not significant when compared to the variability between climate scenarios. Consequently, only the TM soil-water budget was used in the subsequent analyses.

An in-depth description of the development and results from these climate and recharge scenarios can be found in Stigter et al. (2014). The multiple combinations of RCM, bias correction and recharge estimation methods resulted in nine recharge scenarios. Of these, six were selected to be applied in the present study. Calculated total recharge was imposed on the groundwater models as direct recharge. Estimated values of monthly crop water demand (assuming current agricultural area is maintained) was imposed on wells within irrigated areas. Monthly pumping rates measured at public water supply wells during the hydrological year 2006/2007 were applied cyclically, so as to replicate the conditions used by Stigter et al. (2014) with the regional-scale model. A linear sea level rise of 1 m by 2100 was considered at the seaward boundary. Spatial distribution of head (flow model) and sea-water ratio (flow and transport model) obtained from the final time-step of the 2001–2009 model run were used as initial conditions for all climate scenario simulations.

Adaptation scenarios

The following section describes five adaptation measures to increase the QS resilience to climate change. To assess the effect of these measures, simulations are run for a single climate change scenario: ICTP-REGCM3 bias corrected with monthly linear regression (henceforth referred to as ICTP-lin.reg). As will be shown further on, this represents the worst-case scenario in terms of freshwater discharge and extent of SWI. All described scenarios are summarized in Table 2.

The greatest pressure on groundwater is clearly caused by agriculture, due to both large withdrawal volumes as well as the extensive spatial distribution. The first adaptation scenario considers a decrease in groundwater use for irrigation, which could be the result of a combination of adaptation measures such as decreasing irrigated land, increasing agricultural

efficiency or promoting the use of alternative water sources. Two scenarios are considered in which groundwater use for irrigation is decreased by 25 and 50%. A scenario with no groundwater withdrawals for irrigation is simulated to determine the impact of public supply abstraction. Additionally a single model run with no abstraction was also simulated. These last two scenarios are not considered to be realistic adaptation measures, serving merely to determine the impact of reduced recharge and highlight the influence of groundwater users.

The second measure focuses on increasing groundwater supply through managed aquifer recharge (MAR). The ongoing FP7 project, Demonstrating Managed Aquifer Recharge as a Solution to Water Scarcity and Drought (MARSOL), aims to demonstrate MAR as a sound, safe and sustainable strategy that can be applied to optimize water resources management through storage of excess water to be recovered in times of shortage or by influencing gradients. For the QS aquifer, existing large diameter wells would be used to infiltrate surplus water from the large surface water reservoirs currently used for public water supply. Injection and tracer tests have demonstrated the technical feasibility of applying MAR at the location of one such well (Leitão et al. 2014; Costa et al. 2015a, b). An infiltration test demonstrated the capacity to infiltrate 40 m³ in 20 min (equivalent to 1.05×10^6 m³ yr⁻¹). This does not represent the long-term infiltration capacity, but is so far the only measurement for this site. The MAR site is located close to the Alcantarilha water treatment plant (location in Fig. 1), which is supplied by three large surface water dams. At peak capacity, the pipeline can carry 6.74×10^5 m³ d⁻¹; however, at most the treatment plant can process 2.59×10^5 m³ d⁻¹. The unused capacity of the pipeline could be used to transport surplus surface water to be injected into the QS, thus increasing water storage and reducing the SWI. The amount of water available for MAR will thus be constrained by (1) pipeline capacity and (2) surface water availability. Three adaptation scenarios are simulated with continuous injection rates of 1.05, 5.25 and 10.5×10^6 m³ yr⁻¹. The first is the estimated maximum recharge at the single well site already being studied. The latter two values represent a five- and ten-fold increase of the observed infiltration capacity (and coincidentally correspond to approximately 50 and 100% of withdrawals for public water supply), to assess the potential effect of expanding the site.

The third adaptation measure considered is another potential MAR solution to enhance infiltration from streams that cross the QS. There are two main stream networks that cross the QS: the Meirinho stream (West) and the Alte and Algibre streams (east; location in Fig. 1). These intermittent streams bring run-off from the low-permeability Paleozoic rocks north of the system, a portion of which contributes to allogenic recharge, with the remainder (along with some additional base flow from the aquifer system) flowing south towards the sea.

Table 2 Summary of simulated adaptation scenarios

Adaptation measure	Scenario		Δ Abstraction ^a	Δ Recharge ^a	
Decrease groundwater use	No pumping		-45.5	-	
	Irrigation	100% decrease	-35.6	-	
		50% decrease	-17.8	-	
		25% decrease	-8.9	-	
Increase recharge	MAR	Injection in large diameter wells	C1	-	+10.5
			C2	-	+5.3
			C3	-	+1.05
		Enhanced stream infiltration	-	-	+10.9
Spatiotemporal distribution of public-supply abstraction	Spatial	Concentrated (water utility well field)	-	-	-
		Distributed (water utility and municipal well fields)	-	-	-
	Seasonal	Concentrated in dry season	-	-	-
		Concentrated in wet season	-	-	-

^a Average annual change ($\times 10^6 \text{ m}^3 \text{ yr}^{-1}$)

Infiltration of this excess stream flow could be passively enhanced through the use of small dams or weirs and increasing the infiltration capacity of the streambed. Salvador et al. (2012) determined several exponential relationships between average rainfall and the surface water outflow from the area overlying the aquifer taking into account uncertainties in measured stream flow values. These authors estimate that the surface outflow for the Meirinho stream is negligible but average annual outflow from the Alte and Algibre stream network ranges between 16.5×10^6 and $22.6 \times 10^6 \text{ m}^3 \text{ yr}^{-1}$. The most conservative rainfall/surface outflow relationship was applied to the ICTP-lin.reg rainfall series to determine how much excess streamflow could potentially be available for MAR from the Alte and Algibre streams. This relationship may no longer be representative under future climate conditions; however, it serves as an initial estimate. A simulation was run considering all the excess as added recharge along the streams, which on average accounts for an additional recharge of $10.9 \times 10^6 \text{ m}^3 \text{ yr}^{-1}$.

To study the impact of spatial spreading of groundwater abstractions, the baseline model run using the ensemble of climate scenario simulations was compared to one where the abstraction for public water supply in the QS was concentrated in the AdA (water utility) well field. The baseline model run considers abstraction for public supply from both AdA and municipal well fields. This approach does not represent current management practises, but was chosen in order to replicate the simulations by Stigter et al. (2014). Effectively, the distribution of abstraction over several well fields represents a potential adaptation measure in which the negative effects of exploitation are dispersed (Hugman et al. 2012). To study the effect of this measure, a single model run with a public supply abstraction of $9.85 \times 10^6 \text{ m}^3 \text{ yr}^{-1}$ (total public water supply withdrawals in the western sector of the QS) applied entirely to the AdA well field is simulated.

Finally, the fifth adaptation measure is a seasonal distribution of abstraction, by concentrating public supply abstraction during the winter period. As with the spatial distribution, this does not represent current pumping schemes but is representative of a scenario in which the integrated management of surface and groundwater sources of supply allows for a more efficient water resource use. In practice, withdrawals are concentrated during the months in which groundwater levels are already lowest, increasing the risk of short-term negative effects (e.g. insufficient freshwater discharge to GDE). Distributing withdrawals over the year, or even concentrating them during the periods of high water levels, not only reduces this risk but reduces the amount of freshwater which would otherwise be “lost” to the sea. This of course raises other issues, such as what to do with unused surface water during the wet season; however, the point here is to assess whether reducing the seasonality of abstraction contributes to reducing SWI.

Results and discussion

2D cross section model: 2001–2010

The density-coupled model provides a good fit to observed variations in hydraulic head between 2001 and 2009 (Fig. 5). Results provide an improvement on previous models of the QS (i.e. Hugman et al. 2012; Salvador et al. 2012), as they more accurately represent the drawdowns observed during the 2004/2005 drought. This was achieved by increasing withdrawals for irrigation two-fold during the drought years, which highlights the need for a better understanding of the temporal variability of water demand and recharge rates. To achieve a similar result with the regional-scale flow model, a five-fold increase was necessary. This can be due to several reasons: (1) increasing abstraction in the cross section model

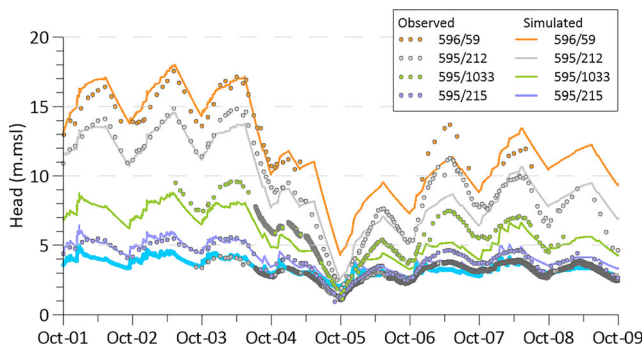


Fig. 5 Observed and simulated hydraulic head time-series at selected monitoring wells (location in Fig. 1)

does not induce more recharge from the north, which occurs in the regional model; (2) different spatial distribution of *T* in the two models; and/or (3) effect of the freshwater–saltwater interface, which reduces the rate of flow from the estuary BC.

Simulated discharge rate at the coastal boundary also follow measured variation in flow rates at springs along the Arade estuary (Fig. 6). Model results are significantly higher, as measured values only represent the sum of flow at several springs and do not take into account diffuse seepage or un-monitored springs. The comparison between total discharge and flow into the model domain along the coastal boundary shown in Fig. 6 shows that during a brief period at the end of the 2004/2005 drought, there was more saltwater entering the system, than there was discharge. This does not mean that no freshwater discharge occurred along the boundary, but merely that the overall balance was towards seawater intrusion.

Simulated chloride concentration in groundwater discharged at the Estombar springs is representative of observed inter-annual variation at the springs and observation wells in the vicinity, but fails to represent seasonal fluctuations (Fig. 7). Both observed and simulated chloride concentrations increase most at the end of 2005 and remain elevated in the subsequent years. Two simulations were run with porosity at the extreme

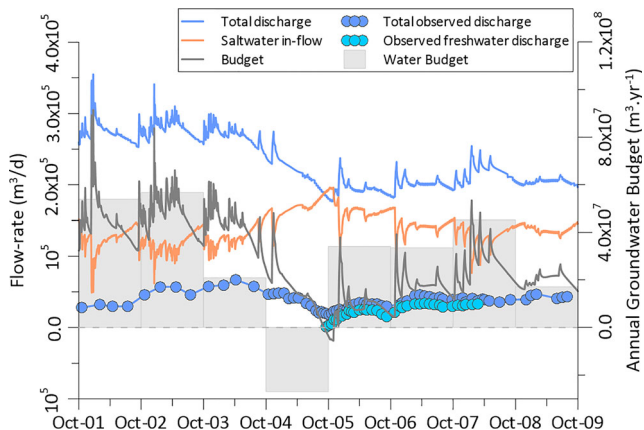


Fig. 6 Comparison between measured discharge at springs and simulated flows through the Arade estuary boundary condition

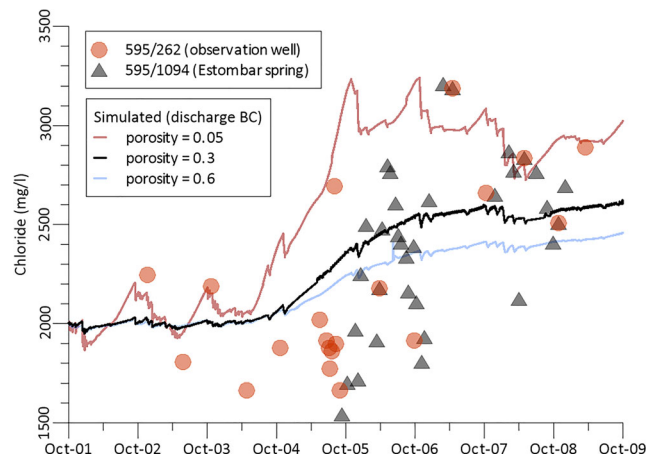


Fig. 7 Comparison between time series of chloride concentration observed at well 595/262 and simulated discharge to the estuary

range of physically acceptable values (0.05 and 0.6) to highlight the parameters effect. Lower values of porosity do in fact lead to slightly faster changes in spring salinity, but in this case over-estimate the observed inter-annual increase. In practice, it is likely that spring flow is associated with highly conductive karst channels with rapid changes in water quality, and the EPM model does not provide an adequate tool to simulate the local-scale processes.

Due to a lack of data on the three-dimensional distribution of the freshwater–saltwater interface, the simulated spatial distribution of saltwater cannot be validated. Available data mostly include measurements from springs, shallow wells and some boreholes, which do not provide a comprehensive image of the variation of salinity with depth. Figure 8 shows that inter-annual variability can have a significant effect on SWI for systems with low porosity by affecting the time-scale at which intrusion occurs. Although the difference between 0.3 and 0.6 is not very significant, results for the simulation with 0.05 show SWI extending over a kilometre further inland, with a significantly thicker transition zone. Low porosity systems are thus more vulnerable to impacts of extreme events such as droughts or to more intense seasonal fluctuation. The effect of hydraulic conductivity and storage parameters on the time-scale of SWI processes is well documented (e.g. Souza and Voss 1987; Watson et al. 2010); however, no assessments of the impact of porosity on the transient nature of the freshwater–saltwater interface were found in the literature. These results show that the area affected by SWI can be underestimated if seasonal and inter-annual variability is ignored, in particular for systems with low porosity, high permeability and low storage. By including temporal variability, the freshwater–saltwater interface reaches further inland during the dry period and is subsequently moves back during the wet period. The additional area affected during the dry period would be ignored in a model that considered constant conditions.

Assuming that a porosity of 0.3 is representative based on simulated chloride concentration in spring discharge and

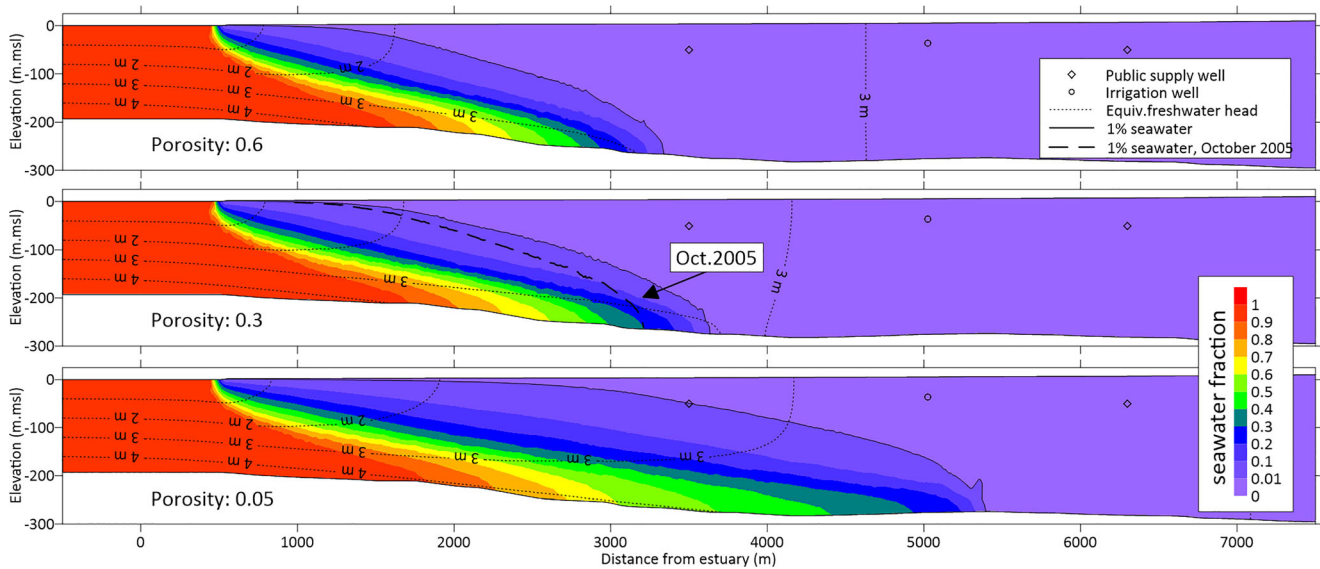


Fig. 8 Comparison of the effect of porosity on the simulated extent of seawater intrusion and freshwater head for October 2009

extent of SWI (Fig. 8), by the end of the simulated period the saltwater interface has yet to reach any significant well fields (Fig. 8, middle). Despite the reduction in abstraction and increase in recharge after 2005 (and subsequent recovery in groundwater levels and discharge), the toe continues to move in-land up until the end of the simulated period, although at a slower pace. These results agree with those of Michael et al. (2005), who observed large-scale saline discharge as a result of seasonal movement of the freshwater–saltwater interface driven by, but lagging behind, seasonal recharge. In the case of the QS during the simulated period, the high inter-annual variability in recharge and abstraction appears to have a greater impact on the interfaces movement than the seasonal fluctuations. This explains the continued high salinity in spring discharge in the three years after the drought in 2004/2005, as groundwater salinity continues to increase near the coast. As was shown in Fig. 4, chloride concentrations in spring discharge only decrease after the year 2009–2010, after a period of very intense recharge. Unfortunately, this is not included in the model as input data was not available at the time of model development.

Climate change scenarios: 2010–2099

The range of simulated total discharge and (seawater) in-flow rates at the coastal boundary from all climate change scenarios are shown in Fig. 9. Results for the ICTP-REGCM3 (linear regression bias-corrected) climate scenario are highlighted for comparison. As is to be expected, simulated discharge (Fig. 9) show the same inter-annual and seasonal variations as obtained by Stigter et al. (2014). Discharge rates from the cross-section model are consistently higher than from the regional model, as they include a portion of recirculated seawater. Results show the largest variation between climate scenarios

occurring in the near future (between 2020 and 2050) with a decreasing range of simulated results towards the end of the century. In part, this is due to the greater number of simulations, as anomaly bias-corrected climate scenarios only span the years 2020–2050 and 2069–2099, and thus the range of simulated values tends to be larger during these periods. Furthermore, as initial conditions for the 2069–2099 anomaly corrected scenarios are based on values from the end of the 2050, the effect of variations in the interim are removed, which increases the uncertainty of the results. Even so, the convergence of all scenarios is unlikely to be a consequence of artefacts of the groundwater model and is most likely attributable to climate predictions. As previously discussed by Stigter et al. (2014), the long-term climate signal becomes stronger than the seasonal and short-term variability. Similar results were obtained by Goderniaux et al. (2011), who showed that despite consistently large confidence intervals around projected groundwater levels, the climate change signal becomes stronger than that of natural climate variability by 2085.

There is a slight increase in in-flow for all (linear regression) scenarios up to 2020; however, between 2020 and 2050, discharge and in-flow rates do not show an overall trend. During the first half of the century only the ICTP-lin.reg scenario shows occurrences of less discharge than in-flow, as simulated during the 2004/2005 drought. These match hydraulic head gradient inversions identified by Stigter et al. (2014). Regular occurrences ensue for several scenarios from the 2060s forward, even over several consecutive years. This coincides with a general decrease in discharge rates across all scenarios. The ICTP-lin.reg climate scenario usually presents the lowest discharge and highest in-flow rates and was therefore selected to simulate adaptation measure scenarios.

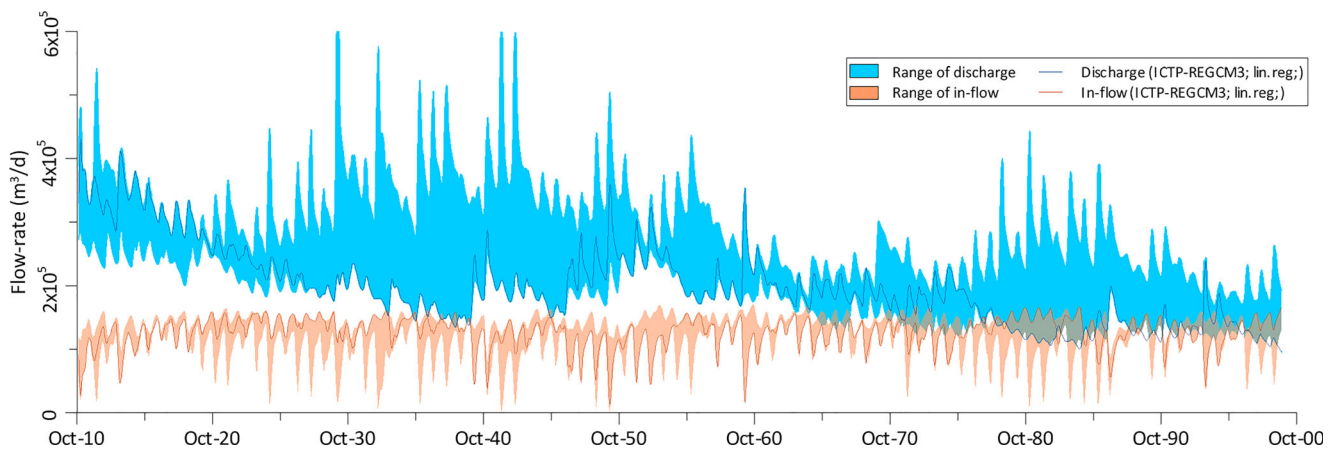


Fig. 9 Ensemble of simulated discharge and seawater in-flow rates at the coastal boundary

The extent of seawater encroachment simulated for the ensemble of climate scenarios (Fig. 10) reflects the range of uncertainty inherent to the climate models. Depending on the climate scenario, by 2050 the position of the freshwater–saltwater ranges between receding 500 m to encroaching 2 km inland. The majority of the scenarios show the interface at approximately the same location as at the end of 2009, indicating that as long as current groundwater use is maintained there is not a significant risk of SWI in the near future, despite the increased seasonal and inter-annual variability. For the worst-case scenario, only one municipal well field would be potentially at risk along with a small patch of agricultural land.

The main impact during this period will be the concentration of freshwater discharge into shorter periods, reflecting the concentrated recharge periods as discussed by Hugman et al. (2013), which may have impacts on associated GDE. However, increased seasonality in and of itself does not have an immediate effect on SWI in the QS due to the relatively slow movement of the freshwater–saltwater interface. In practice it may lead to changes in groundwater use (as was seen for example during 2004/2005), which can induce significant changes in the systems equilibrium and cause lasting effects.

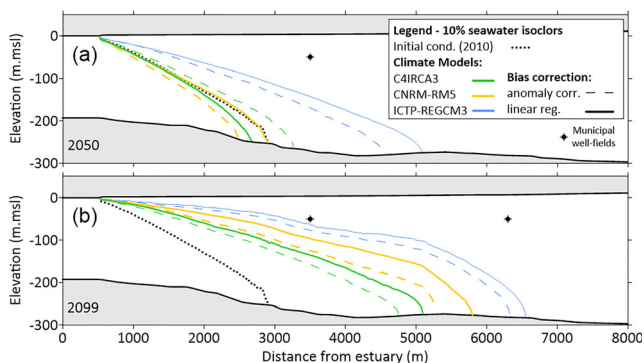


Fig. 10 Comparison of simulated location of the 10% seawater isocline for the ensemble of climate scenarios at the end of the dry season in **a** 2050 and **b** 2099

However, the lack of impact of seasonality on SWI in the QS may not be the case under other hydrogeological conditions. For example, Michael et al. (2005) showed that the interface oscillates seasonally, the extent of which is controlled by a complex function of recharge forcing, aquifer parameters, and location within the aquifer. Thus, depending on local conditions, the area affected by SWI may be substantially underestimated if seasonal effects are ignored.

Predicted reduction in recharge during the second half of the century has a clear impact with significant SWI for all scenarios. The simulations indicate that the freshwater–saltwater interface will move between 2 to 3.5 km further inland. In all cases, the municipal well field nearest to the coast would be contaminated. In the worst-case scenario, saltwater would reach as far inland as the second municipal well field, putting it at risk. Simulated salinity in boreholes up to 6 km from the estuary exceeds usable values for irrigation purposes. Current groundwater use practice would therefore be unsustainable in the long term under this scenario of significantly reduced recharge, with negative impacts to both GDE and human users near the estuary due to the inland movement of the saltwater interface.

Climate change adaptation measures

Comparison between simulated extents of SWI when adaptation measures are considered are shown in Fig. 11. The impact of anthropogenic groundwater use is highlighted by the “no pumping” scenario, in which the freshwater–saltwater interface actually recedes up to 2050 and even in 2099 only slightly exceeds the current in-land extent. The effect of public supply abstraction is relatively small, as demonstrated by the “no irrigation” scenario with almost no change by 2050 and only a slight increase by 2099. In fact, the entire withdrawals for public water supply represent approximately a quarter of the effect of pumping for irrigation. Similar to Hugman et al.

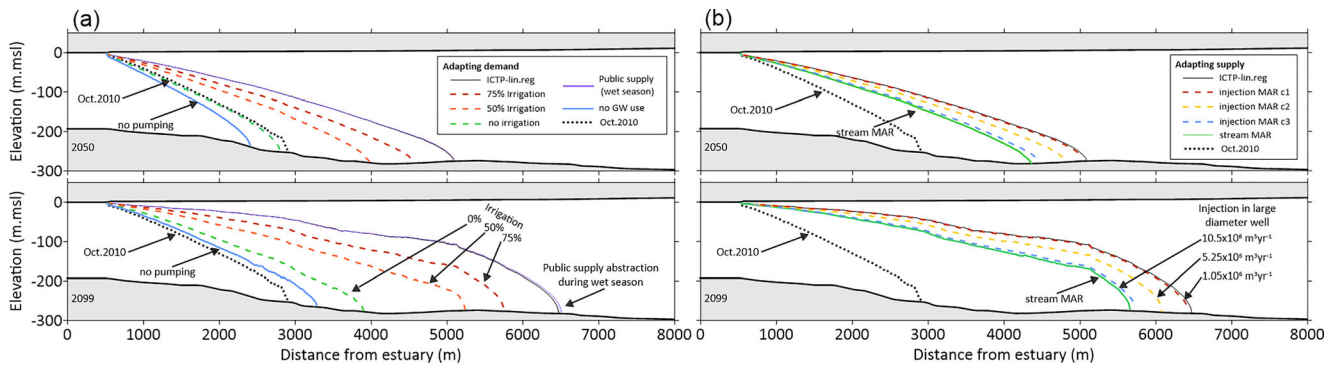


Fig. 11 Comparison of the effect of simulated adaptation measures on the 10% seawater isocline location by **a** 2050 and **b** 2099

(2012), the spatial distribution of public supply withdrawals has a minor effect on the sustainable yield, with only a very slight effect on the extent of the saltwater toe by 2099. As the seasonal effect of abstraction for irrigation greatly outweighs that of public supply, the effect of seasonal optimization of abstraction for public supply on both extent of SWI and discharge rates is practically indistinguishable. Previously Hugman et al. (2013) showed that seasonal optimization of groundwater use had a significant impact on sustainable yield; however, their analysis assumed that all abstraction (public supply and irrigation) would be optimized. The results obtained here suggest that for SWI this is only the case when a significant portion of abstraction is optimized.

Most significant results are obtained by substantially reducing withdrawals for irrigation, as these represent the greatest pressure on the system. Stigter et al. (2013) suggest that the most likely socio-economic development scenario for the area would lead to a decrease in irrigation water demand of approximately $8 \times 10^6 \text{ m}^3 \text{ yr}^{-1}$. This roughly coincides with the scenario in which withdrawal for irrigation is reduced by 25% (average reduction of $8.9 \times 10^6 \text{ m}^3 \text{ yr}^{-1}$); however, even so this level of abstraction would not be sustainable for the worst-case climate scenario simulated here, as the freshwater–saltwater interface moves in-land almost 1.5 km affecting a municipal well field and irrigation wells.

Comparing the relative volumes used for irrigation, public water supply and increased infiltration in Fig. 12 and the respective simulations (Fig. 11), shows that the extent of SWI is directly related to the overall water budget of the system. Reducing irrigation withdrawals by 25 and 50% reduce the extent of SWI by approximately 500 and 1000 m, respectively. Excess stream flow, as well as the $10.5 \times 10^6 \text{ m}^3 \text{ yr}^{-1}$ injection scheme, represent on average 30% of annual irrigation demand (Fig. 12), and have similar effects on the extent of SWI as reducing irrigation withdrawals by 25%. In a similar fashion, the model run including solely public supply withdrawals (which correspond to 25–30% of irrigation demand) cause approximately the same change in extent of SWI. An increase of $10 \times 10^6 \text{ m}^3 \text{ yr}^{-1}$ in the groundwater budget roughly coincides with a decrease of 500 m in the extent of SWI.

In the specific case of the QS, if the sole criteria for sustainability is the extent of SWI, then the long-term groundwater budget provides a useful estimate of the sustainable yield of the system. The results for the no-pumping scenario show that if the current (c.a. 2010) position of the freshwater–saltwater interface is to be maintained, then an average annual discharge of $50 \times 10^6 \text{ m}^3 \text{ yr}^{-1}$ (average annual recharge from 2080 to 2099) must be maintained. This is significantly higher than the $30 \times 10^6 \text{ m}^3 \text{ yr}^{-1}$ (30% of current mean annual recharge) estimated by previous authors (Hugman et al. 2012; Stigter et al. 2014) and the $10 \times 10^6 \text{ m}^3 \text{ yr}^{-1}$ (10% of current mean annual recharge) defined by INAG (2005). Results provided here suggest that these abstraction rates would cause the freshwater–saltwater interface to move inland roughly 1 and 2 km respectively, affecting at least one municipal well field. Current results are insufficient to define the scale at which the sustainable yield needs to be defined. Future work should address this issue, to aid in defining what could be referred to as sustainable levels of groundwater mining (e.g. over-exploiting during short periods) such as occurred during the 2004/2005 drought.

The impact on SWI of current groundwater abstraction for public water supply could be mitigated by either of the simulated MAR solutions; however, there are large differences between the two solutions in terms of their impacts on groundwater levels in the north-eastern sector of the QS (Fig. 13). Additional stream infiltration raises water levels in the north-eastern sector of the QS significantly. Although average

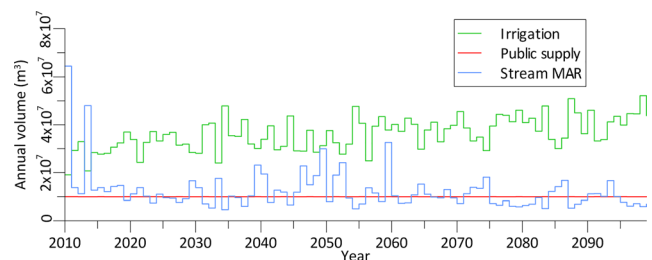


Fig. 12 Simulated annual withdrawals for irrigation and public supply and enhanced stream infiltration for climate scenario ICTP-lin.reg

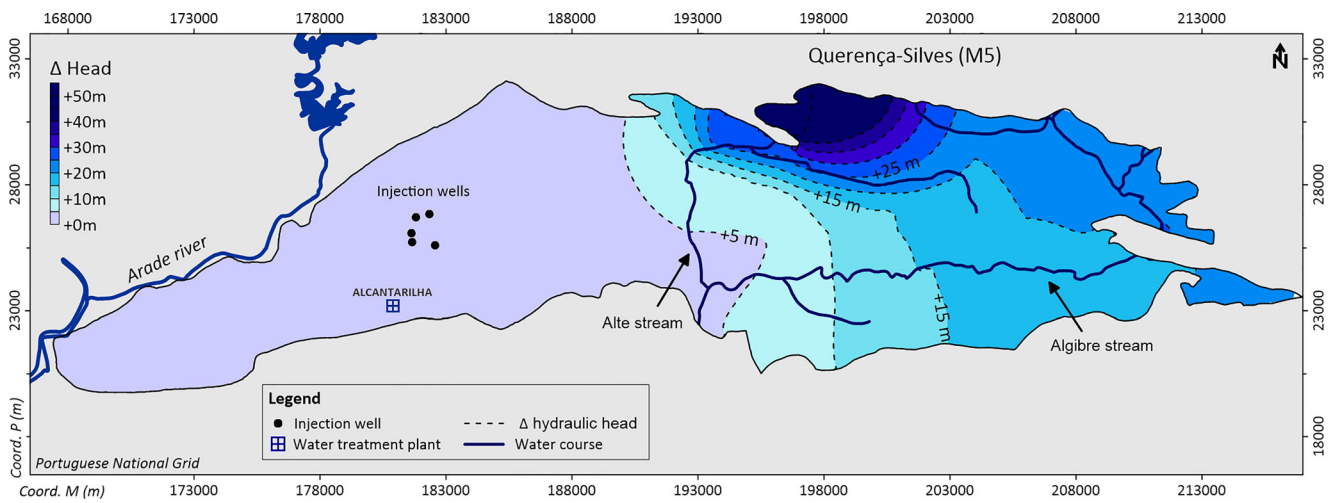


Fig. 13 Difference between simulated hydraulic head at the end of 2099 for the stream infiltration and C1 injection MAR schemes

annual recharge for the simulated period is similar to those of the C1 injection scheme (injection of $10.5 \times 10^6 \text{ m}^3 \text{ yr}^{-1}$ in large diameter wells), recharge during high rainfall years is stored in the eastern sector. This increased storage provides a buffer of discharge to the western sector as well as a larger reserve of freshwater, increasing the aquifers resilience to short-term extreme events and providing source of water supply.

The alternative of using large diameter wells to infiltrate surplus water from the reservoirs is a feasible solution to reduce the risk of SWI, as long as a significant amount of excess surface water can be maintained. As this scheme would require significant investment in terms of infrastructure, a comprehensive assessment of available surplus and the capacity to maintain MAR under future climate conditions is required. Although a comprehensive cost/benefit analysis has yet to be carried out, it is likely that implementing the stream infiltration scheme would be significantly easier from a technical and financial perspective. On the other hand, the estimated excess stream flow is subject to a large amount of uncertainty and values applied here do not take into account the need to maintain ecological flows in the streams nor the practical issues of implementing such a scheme.

Final remarks

Simulations using a coupled-density groundwater flow and transport model demonstrated the effect of predicted changes in recharge, crop water demand and adaptation scenarios on SWI in the QS aquifer system. By considering several climate models, bias correction and recharge calculation methods a degree of uncertainty was included in the results. Uncertainty related to climate change models is evident in the short-term results (2050), with simulated scenarios ranging from a decrease (0.5 km) in SWI to a significant increase (2 km) in

SWI. Changes in rainfall regimes will have an immediate effect on the seasonal variation of discharge; however, the effect on SWI in the QS is attenuated by the freshwater–saltwater interfaces' comparatively slow rate of movement.

In the long-term, the scenarios converge. All simulations show significant increase (between 2 to 3.5 km) in SWI by the end of the century. Despite predicted encroachment of the freshwater–saltwater interface, simulations indicate that public water supply wells managed by the regional water utility are not under risk of salinization if current water management practises are maintained. However, users within 6 km of the coast will be adversely affected. These include several agricultural areas and two municipal well fields currently maintained as reserves to supplement public water supply, as well as the estuarine GDE. Adaptation measures will be necessary to maintain current groundwater quality in the long term.

Comparing the effects of proposed adaptation measures confirms that the extent of SWI in the QS is controlled by the long-term water budget. The effectiveness of both demand (e.g. reduced withdrawals, alternative sources, optimized spatiotemporal abstraction) and supply (managed aquifer recharge) oriented measures on the extent of SWI is directly related to the change in water budget. However, this is specific to SWI and ignores other sustainability criteria, such as maintaining ecological flows to GDE. Taking these issues into account, the single most effective measure would be a MAR scheme to increase infiltration of run-off from the Palaeozoic rocks north of the system, which would counteract the effect of decreasing recharge from climate change. Research is required to better understand the surface/groundwater interactions in this system, as well as estimate the effects of climate change on surface-water availability, in order to assess the practical feasibility of either MAR scheme.

Previous authors (Hugman et al. 2013) estimated sustainable yield for the QS as 70% of the mean annual recharge, in order to maintain freshwater discharge at the Estombar

springs; however, the impact on SWI and the salinization of spring discharge was not taken into account. Current results show that these latter two criteria are mostly controlled by the long-term water budget of the system, and that previously proposed sustainable yields would lead to the salinization of several public supply and irrigation wells. Therefore, to maintain both current ecological status of the GDEs and groundwater quality, mean annual discharge should be in the order of $50 \times 10^6 \text{ m}^3 \text{ yr}^{-1}$ (ca. 50% of current mean annual recharge). Further work is required to define the time-scale for which this sustainable yield can be defined and how it relates to the physical parameters of a given system.

Acknowledgements The first author wishes to acknowledge the Fundação para a Ciência e Tecnologia (FCT) for the PhD grant SFRH/BD/80149/2011, as well as DHI for supplying a student licence of the FEFLOW software. The research leading to these results has also received funding from the European Union Seventh Framework Programme (FP7/2007-2013) under grant agreement No. 619120 (Demonstrating Managed Aquifer Recharge as a Solution to Water Scarcity and Drought – MARSOL).

Appendix: abbreviations

AdA	Águas do Algarve [regional water utility]
BC	Boundary condition
EPM	Equivalent porous medium
FAO	Food and Agriculture Organization
GCM	Global circulation model
GDE	Groundwater dependent ecosystem
ICTP-lin.reg	ICTP-REGCM3 climate scenario, bias corrected with monthly linear regression
MAR	Managed aquifer recharge
PG	Penman-Grindley
QS	Querença-Silves
RCM	Regional climate model
SGD	Submarine groundwater discharge
SWI	Seawater intrusion
TM	Thornthwaite-Mather

References

- Abarca E, Carrera J, Sánchez-Vila X, Voss CI (2007) Quasi-horizontal circulation cells in 3D seawater intrusion. *J Hydrol* 339:118–129. doi:10.1016/j.jhydrol.2007.02.017
- Almeida C, Mendonça JLL, Jesus MR, Gomes AJ (2000) Sistemas Aquíferos de Portugal Continental [Aquifer systems in continental Portugal]. INAG, Lisbon
- Bear J (1972) Dynamics of fluids in porous media. American Elsevier, New York
- Burnett WC, Aggarwal PK, Aureli A et al (2006) Quantifying submarine groundwater discharge in the coastal zone via multiple methods. *Sci Total Environ* 367:498–543. doi:10.1016/j.scitotenv.2006.05.009
- Carneiro JF, Boughriba M, Correia A et al (2010) Evaluation of climate change effects in a coastal aquifer in Morocco using a density-dependent numerical model. *Environ Earth Sci* 61:241–252. doi:10.1007/s12665-009-0339-3
- Chang SW, Clement TP (2012) Experimental and numerical investigation of saltwater intrusion dynamics in flux-controlled groundwater systems. *Water Resour Res* 48, W09527. doi:10.1029/2012WR012134
- Chang SW, Clement TP, Simpson MJ, Lee K-K (2011) Does sea-level rise have an impact on saltwater intrusion? *Adv Water Resour* 34:1283–1291. doi:10.1016/j.advwatres.2011.06.006
- Costa L, Monteiro JP, Oliveira M et al (2015a) Modelling contributions of the local and regional groundwater flow of managed aquifer recharge activities at Querença-Silves aquifer system. *EGU Gen. Assem.* 2015, P 11930, Vienna, 12–17 April 2015
- Costa LRD, Monteiro JP, Oliveira MM, et al (2015b) Interpretation of an injection test in a large diameter well in south Portugal and contribution to the understanding of the local hydrogeology. 10 Semin. Sobre Águas Subterrâneas 10, APRH, Evora, Portugal, April 2015, pp 2013–2016
- Custodio E (2002) Aquifer overexploitation: what does it mean? *Hydrogeol J* 10:254–277. doi:10.1007/s10040-002-0188-6
- Diersch HJG (2014) FEFLOW: finite element modeling of flow, mass and heat transport in porous and fractured media. doi:10.1007/978-3-642-38739-5
- Diersch H-JG, Kolditz O (1998) Coupled groundwater flow and transport: 2. thermohaline and 3D convection systems. *Adv Water Resour* 21:401–425. doi:10.1016/S0309-1708(97)00003-1
- Doherty J (2002) Model-independent parameter estimation, 4th edn. Watermark, Brisbane, Australia
- Estrela T, Marcuello C, Iglesias A (1996) Water resources problems in southern Europe. Copenhagen, Denmark
- Ferguson G, Gleeson T (2012) Vulnerability of coastal aquifers to groundwater use and climate change. *Nat Clim Chang* 2:342–345. doi:10.1038/nclimate1413
- Gelhar LW, Welty C, Rehfeldt KR (1992) A critical review of data on field-scale dispersion in aquifers. *Water Resour Res* 28:1955–1974. doi:10.1029/92WR00607
- Giorgi F (2006) Climate change hot-spots. *Geophys Res Lett* 33:L08707. doi:10.1029/2006GL025734
- Goderniaux P, Brouyère S, Blenkinsop S et al (2011) Modeling climate change impacts on groundwater resources using transient stochastic climatic scenarios. *Water Resour Res* 47, W12516. doi:10.1029/2010WR010082
- Green NR, MacQuarrie KTB (2014) An evaluation of the relative importance of the effects of climate change and groundwater extraction on seawater intrusion in coastal aquifers in Atlantic Canada. *Hydrogeol J* 22:609–623. doi:10.1007/s10040-013-1092-y
- Green TR, Taniguchi M, Kooi H et al (2011) Beneath the surface of global change: impacts of climate change on groundwater. *J Hydrol* 405:532–560. doi:10.1016/j.jhydrol.2011.05.002
- Holman IP (2006) Climate change impacts on groundwater recharge: uncertainty, shortcomings, and the way forward? *Hydrogeol J* 14:637–647. doi:10.1007/s10040-005-0467-0
- Holman IP, Allen DM, Cuthbert MO, Goderniaux P (2012) Towards best practice for assessing the impacts of climate change on groundwater. *Hydrogeol J* 20:1–4. doi:10.1007/s10040-011-0805-3
- Hugman R, Stigter TY, Monteiro JP (2013) The importance of temporal scale when optimising abstraction volumes for sustainable aquifer exploitation: a case study in semi-arid South Portugal. *J Hydrol* 490:1–10. doi:10.1016/j.jhydrol.2013.02.053
- Hugman R, Stigter TY, Monteiro JP, Nunes L (2012) Influence of aquifer properties and the spatial and temporal distribution of recharge and abstraction on sustainable yields in semi-arid regions. *Hydrol Process* 26:2791–2801. doi:10.1002/hyp.8353
- INAG (2005) Relatório Síntese Sobre a Caracterização das Regiões Hidrográficas Prevista na Directiva-Quadro da Água [Report on

- the characterization of the hydrographic regions as per the Water Framework Directive]. INAG, Lisbon, Portugal
- IPCC (2014) Climate change 2014: impacts, adaptation, and vulnerability—part A, global and sectoral aspects. Contribution of Working Group II to the Fifth Assessment Report of the Intergovernmental Panel on Climate Change. IPCC, Geneva. doi: [10.1016/j.renene.2009.11.012](https://doi.org/10.1016/j.renene.2009.11.012)
- Jackson CR, Meister R, Prudhomme C (2011) Modelling the effects of climate change and its uncertainty on UK chalk groundwater resources from an ensemble of global climate model projections. *J Hydrol* 399:12–28. doi: [10.1016/j.jhydrol.2010.12.028](https://doi.org/10.1016/j.jhydrol.2010.12.028)
- Kiraly L (1975) Rapport sur l'état actuel des connaissances dans le domaine des caractères physiques des roches karstiques [Report on the present knowledge on the physical characteristics of karstic rocks]. In: Burger A, Dubertret L (eds) Hydrogeology of karstic terrains. International Association of Hydrogeologists (IAH), Paris, France, pp 53–67
- Kolditz O, Ratke R, Dierschb HG, Zielke W (1998) Coupled groundwater flow and transport: 1. verification of variable density flow and transport models. *Adv Water Resour* 21(1):27–46
- Kopsiaftis G, Mantoglou A, Giannouloupoulos P (2009) Variable density coastal aquifer models with application to an aquifer on Thira Island. *Desalination* 237:65–80. doi: [10.1016/j.desal.2007.12.023](https://doi.org/10.1016/j.desal.2007.12.023)
- Leitão TE, Lobo-Ferreira JP, Carvalho T et al (2014) MARSOL : demonstrating managed aquifer recharge as a solution to water scarcity and drought. 10th Semin. Sobre Águas Subterrâneas, APRH, Evora, Portugal, April 2015, 4 pp
- Loáiciga HA, Pingel TJ, Garcia ES (2012) Sea water intrusion by sea-level rise: scenarios for the 21st century. *Ground Water* 50:37–47. doi: [10.1111/j.1745-6584.2011.00800.x](https://doi.org/10.1111/j.1745-6584.2011.00800.x)
- Manuppella G (1992) Notícia Explicativa da Carta geológica da região do Algarve (escala 1/100000) [Explanatory note of the geological map of the Algarve region (scale 1/100000)]. Serv Geol Portugal, Lisbon
- MED-EUWI (2007) Mediterranean groundwater report: technical report on groundwater management in the Mediterranean and the Water Framework Directive. MED-EUWI, Athens
- Michael HA, Mulligan AE, Harvey CF (2005) Seasonal oscillations in water exchange between aquifers and the coastal ocean. *Nature* 436: 1145–1148. doi: [10.1038/nature03935](https://doi.org/10.1038/nature03935)
- Monteiro JP, Costa MS (2004) Dams, groundwater modelling and water management at the regional scale in a coastal Mediterranean area (the southern Portugal region—Algarve). *Larhyss J* 3:157–169
- Monteiro JP, Oliveira MM, Costa JP (2007a) Impact of the replacement of groundwater by dam waters in the Albufeira-Ribeira de Quarteira and Quarteira coastal aquifers. XXXV AIH Congr. Groundw. Ecosyst. Lisbon, Portugal, September 2007, pp 489–490
- Monteiro JP, Ribeiro L, Martins J (2007b) Modelação Matemática do Sistema Aquífero Querença-Silves. Relatório Final. Validação e Análise de Cenários Relatório Técnico [Mathematical modelling of Querença-Silves Aquifer System. Final report. Validation and scenario analysis] Technical report, Instituto Superior Técnico, Lisbon, Portugal
- Monteiro JP, Vieira J, Nunes L, Younes F (2006) Inverse calibration of a regional flow model for the Querença-Silves Aquifer System. Int. Congr. Integr. Water Resour. Manag. Challenges Sustain. Dev. Marrakesh, Morocco, May 2006, 44 pp
- Neuman SP (2005) Longitudinal dispersivity data and implications for scaling behavior. *Ground Water* 44:139–140. doi: [10.1111/j.1745-6584.2006.00166.x](https://doi.org/10.1111/j.1745-6584.2006.00166.x)
- Neves MC, Costa L, Monteiro JP (2016) Climatic and geologic controls on the piezometry of the Querença-Silves karst aquifer, Algarve (Portugal). *Hydrogeol J* 24:1015–1028. doi: [10.1007/s10040-015-1359-6](https://doi.org/10.1007/s10040-015-1359-6)
- Nocchi M, Salleolini M (2013) A 3D density-dependent model for assessment and optimization of water management policy in a coastal carbonate aquifer exploited for water supply and fish farming. *J Hydrol* 492:200–218. doi: [10.1016/j.jhydrol.2013.03.048](https://doi.org/10.1016/j.jhydrol.2013.03.048)
- Nunes G, Monteiro JP, Martins J (2006) Quantificação do consumo de água subterrânea na agricultura por métodos indirectos: detecção remota [Indirect methods for quantifying agricultural groundwater use: remote detection]. In: ESIG (ed) Proc. IX Encontro Util. Informação Geográfica. Oeiras, Portugal, November 2006, 15 pp
- Oliveira MM, Oliveira L, Ferreira JPL (2008) Estimativa da recarga natural no sistema aquífero de Querença-Silves (Algarve) pela aplicação do modelo BALSEQ_MOD [Estimation of natural recharge in the Querença-Silves aquifer system (Algarve)]. Proc. 9th Congr. da Água. Cascais, Portugal, May 2008, 15 pp
- Oude Essink G (2001) Saltwater intrusion in 3D large scale aquifers: a Dutch case. *Phys Chem Earth* 26:337–344
- Oude Essink GHP, van Baaren ES, de Louw PGB (2010) Effects of climate change on coastal groundwater systems: a modeling study in the Netherlands. *Water Resour Res* 46, W00F04. doi: [10.1029/2009WR008719](https://doi.org/10.1029/2009WR008719)
- Papadopoulou MP, Varouchakis EA, Karatzas GP (2010) Terrain discontinuity effects in the regional flow of a complex karstified aquifer. *Environ Model Assess* 15(5):319–328. doi: [10.1007/s10666-009-9207-5](https://doi.org/10.1007/s10666-009-9207-5)
- Payne DF (2010) Effects of climate change on saltwater intrusion at Hilton Head Island, SC, U.S.A. 21st Salt Water Intrusion Meet 2010, pp 293–296
- Rasmussen P, Sonnenborg TO, Gonciar G, Hinsby K (2012) Assessing impacts of climate change, sea level rise, and drainage canals on saltwater intrusion to coastal aquifer. *Hydrol Earth Syst Sci Discuss* 9:7969–8026. doi: [10.5194/hessd-9-7969-2012](https://doi.org/10.5194/hessd-9-7969-2012)
- Rozell DJ, Wong T (2010) Effects of climate change on groundwater resources at Shelter Island, New York State, USA. *Hydrogeol J* 18:1657–1665. doi: [10.1007/s10040-010-0615-z](https://doi.org/10.1007/s10040-010-0615-z)
- Salvador N, Monteiro JP, Hugman R et al (2012) Quantifying and modelling the contribution of streams that recharge the Querença-Silves aquifer in the south of Portugal. *Nat Hazards Earth Syst Sci* 12: 3217–3227. doi: [10.5194/nhess-12-3217-2012](https://doi.org/10.5194/nhess-12-3217-2012)
- Santos FD, Miranda P (2006) Alterações climáticas em Portugal. Cenários, Impactos e Medidas de Adaptação [Climate change in Portugal: scenarios, impacts and adaptation measures]. Project SIAM II, 1st edn. Gradiva, Lisbon, Portugal
- Scanlon BR, Mace RE, Barrett ME, Smith B (2003) Can we simulate regional groundwater flow in a karst system using equivalent porous media models? Case study, Barton Springs, Edwards aquifer, USA. *J Hydrol* 276:137–158. doi: [10.1016/S0022-1694\(03\)00064-7](https://doi.org/10.1016/S0022-1694(03)00064-7)
- Silva ACF, Tavares P, Shapouri M et al (2012) Estuarine biodiversity as an indicator of groundwater discharge. *Estuar Coast Shelf Sci* 97: 38–43. doi: [10.1016/j.ecss.2011.11.006](https://doi.org/10.1016/j.ecss.2011.11.006)
- Smith AJ, Turner JV (2001) Density-dependent surface water–groundwater interaction and nutrient discharge in the Swan–Canning estuary. *Hydrol Process* 15:2595–2616. doi: [10.1002/hyp.303](https://doi.org/10.1002/hyp.303)
- Souza WR, Voss CI (1987) Analysis of an anisotropic coastal aquifer system using variable-density flow and solute transport simulation. *J Hydrol* 92:17–41. doi: [10.1016/0022-1694\(87\)90087-4](https://doi.org/10.1016/0022-1694(87)90087-4)
- Stigter T, Bento S, Varanda MP et al (2013) Combined assessment of climate change and socio-economic development as drivers of freshwater availability in the south of Portugal. TWAM2013 Int. Conf. Work, Aveiro, Portugal, March 2013
- Stigter TY, Monteiro JP, Nunes LM et al (2009) Screening of sustainable groundwater sources for integration into a regional drought-prone water supply system. *Hydrol Earth Syst Sci Discuss* 6:85–120. doi: [10.5194/hessd-6-85-2009](https://doi.org/10.5194/hessd-6-85-2009)
- Stigter TY, Nunes JP, Pisani B et al (2014) Comparative assessment of climate change and its impacts on three coastal aquifers in the

- Mediterranean. *Reg Environ Chang* 14:41–56. doi:[10.1007/s10113-012-0377-3](https://doi.org/10.1007/s10113-012-0377-3)
- Sulzbacher H, Wiederhold H, Siemon B et al (2012) Numerical modelling of climate change impacts on freshwater lenses on the North Sea Island of Borkum using hydrological and geophysical methods. *Hydrol Earth Syst Sci* 16:3621–3643. doi:[10.5194/hess-16-3621-2012](https://doi.org/10.5194/hess-16-3621-2012)
- Taniguchi M, Burnett WC, Cable JE, Turner JV (2002) Investigation of submarine groundwater discharge. *Hydrol Process* 16:2115–2129. doi:[10.1002/hyp.1145](https://doi.org/10.1002/hyp.1145)
- Taylor RG, Scanlon B, Döll P et al (2012) Ground water and climate change. *Nat Clim Chang* 3:322–329. doi:[10.1038/nclimate1744](https://doi.org/10.1038/nclimate1744)
- van der Linden P, Mitchell JFB (2009) ENSEMBLES: climate change and its impacts: summary of research and results from the ENSEMBLES project. Met Office Hadley Centre, Exeter, UK
- Watson TA, Werner AD, Simmons CT (2010) Transience of seawater intrusion in response to sea level rise. *Water Resour Res* 46:W12533. doi:[10.1029/2010WR009564](https://doi.org/10.1029/2010WR009564)
- Werner AD, Simmons CT (2009) Impact of sea-level rise on sea water intrusion in coastal aquifers. *Ground Water* 47:197–204. doi:[10.1111/j.1745-6584.2008.00535.x](https://doi.org/10.1111/j.1745-6584.2008.00535.x)
- Zheng C, Bennett GD (1995) Applied contaminant transport modeling: theory and practice. Wiley,